Inorganic Chemistry

Article

pubs.acs.org/IC

Crucial Role of Paramagnetic Ligands for Magnetostructural Anomalies in "Breathing Crystals"

Evgeny V. Tretyakov,[†] Svyatoslav E. Tolstikov,[†] Anastasiya O. Suvorova,[†] Aleksey V. Polushkin,[†] Galina V. Romanenko,[†] Artem S. Bogomyakov,[†] Sergey L. Veber,[†] Matvey V. Fedin,[†] Dmitry V. Stass,[‡] Edward Reijerse,[§] Wolfgang Lubitz,[§] Ekaterina M. Zueva,[∥] and Victor I. Ovcharenko*[,†]

[†]International Tomography Center, and [‡]Institute of Chemical Kinetics and Combustion, Siberian Branch of the Russian Academy of Sciences, Institutskaya Street, 630090 Novosibirsk, Russian Federation

[§]Max-Planck-Institut für chemische Energiekonversion, 45470 Mülheim/Ruhr, Germany

[∥]Department of Inorganic Chemistry, Kazan State Technological University, 68 K. Marx Street, 420015 Kazan, Russian Federation

Supporting Information

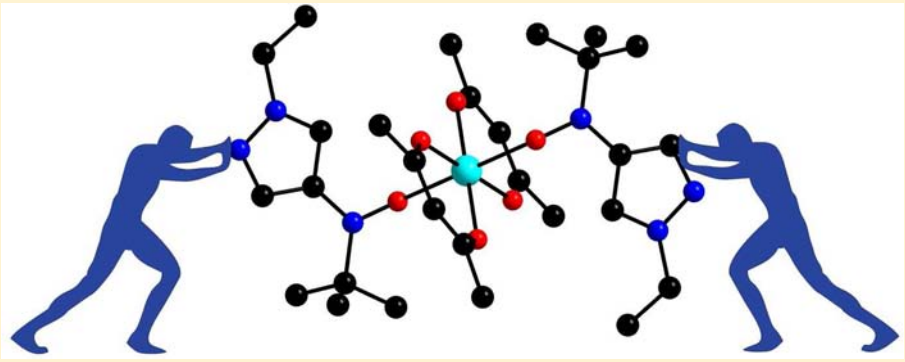

ABSTRACT: Breathing crystals based on polymer-chain complexes of $Cu(hfac)_2$ with nitroxides exhibit thermally and light-induced magnetostructural anomalies in many aspects similar to a spin crossover. In the present work, we report the synthesis and investigation of a new family of $Cu(hfac)_2$ complexes with *tert*-butylpyrazolylnitroxides and their nonradical structural analogues. The complexes with paramagnetic ligands clearly exhibit structural rearrangements in the copper(II) coordination units and accompanying magnetic phenomena characteristic for breathing crystals. Contrary to that, their structural analogues with diamagnetic ligands do not undergo rearrangements in the copper(II) coordination environments. This confirms experimentally the crucial role of paramagnetic ligands and exchange interactions between them and copper(II) ions for the origin of magnetostructural anomalies in this family of molecular magnets.

INTRODUCTION

The synthesis of heterospin complexes of transition metals and nitroxides often involves Cu(II) as the complex-forming metal.[1] Compounds of Cu(II) with nitroxides are valuable model objects for magnetochemical studies because the analysis of their properties does not require the account of spin−orbital contribution.[2] They are also convenient for EPR studies, which were widely used for investigating the first coordination compounds of transition metals with nitroxides.[1a,b] However, the synthesis of heterospin compounds of Cu(II) and multifunctional nitroxides always involves the difficulty of predicting the coordination mode of nitroxide in a solid. This is a multifactor effect, which depends on the acceptor properties of the metal-containing matrix, the steric accessibility of the nitroxyl group, the electronic effects of functional groups other than >N·O in the structure of nitroxide, conditions of synthesis, and packing effects in the resulting solid. The formation of a $Cu-O_{ON}$ coordination bond in the solid complex is an essential condition for the potential polymorphic transformation of the compound.

The majority of known Cu(II) complexes with nitroxides are stable in polymorphic transformations.[1m] On cooling or heating in a wide temperature range, XRD shows very small changes in the geometrical parameters due to crystal compression on cooling or expansion on heating. At the same time, a large group of Cu(II) complexes with nitroxides experience structural rearrangements of heterospin coordination units due to variation of temperature, leading to various magnetic anomalies on the curve of the temperature dependence of the effective magnetic moment (μ_{eff}).[3] This group mainly involves $Cu(hfac)_2$ complexes, where hfac is hexafluoroacetylacetonate, which is a powerful acceptor capable of coordinating the O atom of the O·*N*< fragment with weak

Received: May 31, 2012
Published: August 14, 2012

   dx.doi.org/10.1021/ic301149e | *Inorg. Chem.* 2012, 51, 9385−9394

donor properties comparable to the donor properties of the acetone molecule.[4]

Among heterospin complexes capable of thermally induced magnetic effects are $[Cu(hfac)_2L^R]$ complexes, where L^R are pyrazolyl-substituted nitronylnitroxides. The single crystals of these compounds possess unique mechanical plasticity, due to which they retain their quality in the course of thermally induced phase transitions. Their quality remains high enough for using the same single crystal in a series of experiments on structure determination during polymorphic transformations. Because of this, the structure of a heterospin complex at a definite temperature can be unambiguously correlated with its magnetic characteristics.[5] On the basis of this striking feature, these heterospin complexes were grouped together under the name of breathing crystals.[5c] The ability of $[Cu(hfac)_2L^R]$ crystals to retain their integrity during repeated cooling–heating cycles also allows real-time observation of direct and reverse phase transition waves along the single crystal.

Systematic studies of the relationship between the structural dynamics and the character of variation of the magnetic properties of $[Cu(hfac)_2L^R]$ serve as a basis for quantum-chemical analysis of the electronic structure of exchange channels[6] and the development of theoretical approaches to the analysis and description of spin transitions in heterospin exchange clusters.[7] The spin state dynamics of {>N∴O−Cu^{2+}−O∴*N*<} or {Cu^{2+}−O∴*N*<} exchange clusters also shows itself in a specific way in EPR spectra, providing detailed information about the character of intracluster exchange interactions.[8] Radiospectroscopic studies of breathing crystals revealed a rare (for multispin compounds) situation when interchain exchange interactions were higher in energy than interactions inside the chain.[9] Moreover, the spin state of these compounds can change during photoexcitation, stimulating interest to them in view of their ability to serve as optical magnetic switches.[10]

Coordination of the O∴*N*< group by the copper ion was always considered to be an essential condition for thermally induced structural rearrangements of {>N∴O−Cu^{2+}−O∴*N*<} or {Cu^{2+}−O∴*N*<} heterospin coordination fragments, which, in turn, give rise to anomalies on the $\mu_{eff}(T)$ curve.[1] However, this was not confirmed experimentally because it requires synthesis and further comparative structural and magnetochemical studies of Cu(II) complexes with nitroxides and diamagnetic ligands structurally related to these nitroxides.

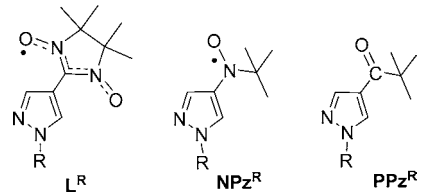

Before this study, attempts to synthesize such pairs of dia- and paramagnetic organic ligands and Cu(II) complexes with a structure of the solid phase similar to each representative of this pair have failed.

In this work, we have succeeded in synthesizing the topological analogues of L^R, nitroxides NPz^R, and their diamagnetic analogues, pivaloylpyrazoles PPz^R. $[Cu(hfac)_2(NPz^R)]$ heterospin complexes having a polymer chain structure in the solid state were isolated, and their magnetic properties were studied. These properties were compared to those of $[Cu(hfac)_2(PPz^R)]$ having a similar structure of polymer chains but containing ketones as the structural diamagnetic analogues of NPz^R. As a result, our studies of $[Cu(hfac)_2(NPz^R)]$ and $[Cu(hfac)_2(PPz^R)]$ provided first unambiguous experimental evidence that the presence of a coordinated nitroxyl fragment in the structure of the heterospin compound is an essential condition for the breathing crystal effect.

RESULTS AND DISCUSSION

Complexes with Nitroxides. The general procedures for the synthesis of paramagnetic ligands NPz^R are given in the Experimental Section. The EPR spectra of NPz^R were quite similar, showing the dominant triplet from the *N*-oxyl nitrogen with a substructure from the nuclei of the pyrazolyl substituent (Figure 1 for NPz^{Me}, and Supporting Information for NPz^{Et}, NPz^{Pr}, and NPz^{Bu}). The substructure involved two relatively strong couplings with protons in the third and fifth positions of the pyrazole ring, weaker couplings with three equivalent methyl protons of the *N*-methyl group in NPz^{Me} or with two equivalent *N*-methylene protons in NPz^R (R = Et, Pr, Bu), and still weaker couplings with pyrazole nitrogens. The EPR spectra of NPz^R indicated a substantial delocalization of spin density to the pyrazolyl substituent, which was further confirmed by DFT calculations (Supporting Information). This distinguishes NPz^R from L^R, in which spin density delocalization to the pyrazole ring is much weaker. This circumstance is important

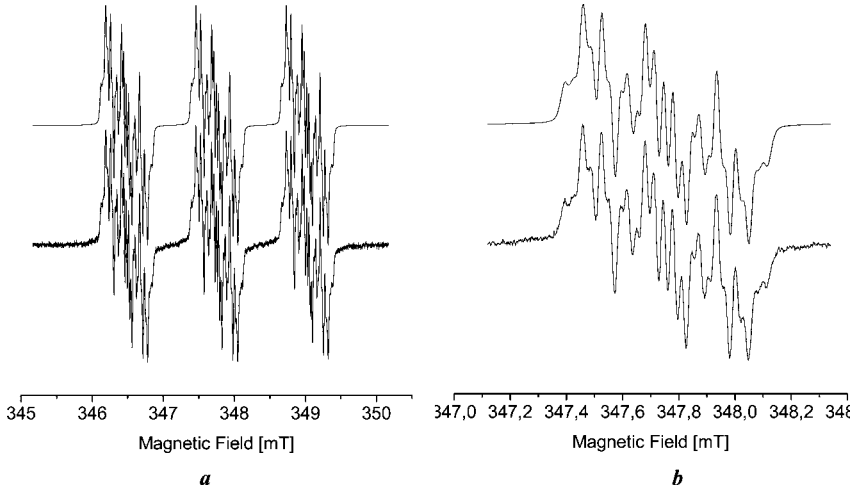

Figure 1. Experimental (noisy trace) and simulated (up-shifted clean trace) EPR spectra for NPz^{Me} (a) and central line (b).

dx.doi.org/10.1021/ic301149e | *Inorg. Chem.* 2012, 51, 9385−9394

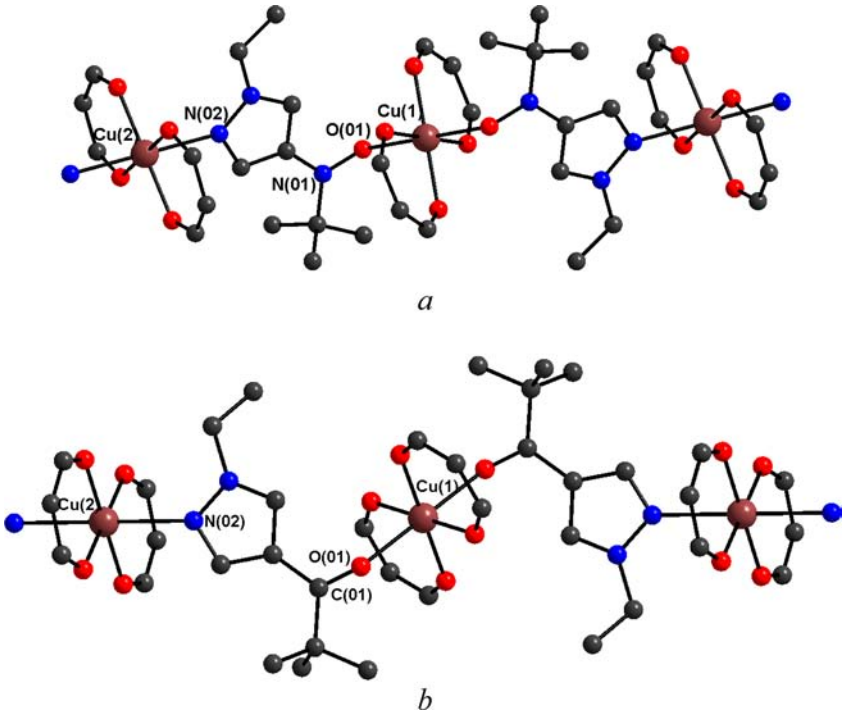

Figure 2. Polymer chain fragment in solid $[Cu(hfac)_2(NPz^{Et})]\cdot 0.5C_7H_{16}$ (a) and $[Cu(hfac)_2(PPz^{Et})]$ (b).

for understanding the magnetic properties of $Cu(hfac)_2$ heterospin complexes with NPz^R.

The $[Cu(hfac)_2(NPz^R)]$ complexes were prepared by the reaction of $Cu(hfac)_2$ with freshly prepared NPz^R in hexane or heptane. After the reagents were mixed, the mother solutions were quickly cooled to −15 °C and stored at this temperature overnight. The resulting crystals of the complexes were separated from the mother solution and also stored at −15 °C. The heating of the complexes, especially to 30−35 °C, stimulated their active decomposition in both liquid and solid states.

Note that when the reaction with NPz^{Me} or NPz^{Et} was performed in heptane, the solid phase of the complexes with a polymer chain structure included the corresponding solvate molecules in case of $[Cu(hfac)_2(NPz^{Me})]\cdot 0.5C_7H_{16}$ or $[Cu(hfac)_2(NPz^{Et})]\cdot 0.5C_7H_{16}$, whereas $[Cu(hfac)_2(NPz^{Pr})]$ and $[(Cu(hfac)_2(NPz^{Bu})]$ did not contain solvate molecules. The mass of the finely crystalline compounds $[Cu(hfac)_2(NPz^{Pr})]$ or $[(Cu(hfac)_2(NPz^{Bu})]$ included large individual crystals of two polymorphic modifications of $[(Cu(hfac)_2)_3(NPz^{Pr})_2]$ or $[(Cu(hfac)_2)_3(NPz^{Bu})_2]$ trinuclear complexes (Supporting Information). The introduction of an additional amount of NPz^{Pr} or NPz^{Bu} in the reaction mixture did not suppress the formation of trinuclear complexes. During crystallization of complexes from the hexane solution, all compounds were obtained as solvates $[Cu(hfac)_2(NPz^R)]\cdot 0.5C_6H_{14}$ (R = Me, Et, Pr, Bu). An X-ray diffraction study of $[Cu(hfac)_2(NPz^R)]\cdot 0.5C_7H_{16}$ (R = Me, Et) and $[Cu(hfac)_2(NPz^R)]\cdot 0.5C_6H_{14}$ (R = Me, Et, Pr, Bu) was performed for crystals separated from the layer of the mother solution and then coated with a layer of epoxide resin. When isolated from the mother solution, the $[Cu(hfac)_2(NPz^{Me})]\cdot 0.5C_7H_{16}$ and $[Cu(hfac)_2(NPz^R)]\cdot 0.5C_6H_{14}$ solvates (R = Me, Pr, Bu) quickly lost the included solvent molecules. The $[Cu(hfac)_2(NPz^{Et})]\cdot 0.5C_7H_{16}$ and $[Cu(hfac)_2(NPz^{Et})]\cdot 0.5C_6H_{14}$ complexes were kinetically stable enough; therefore, they were easy to study.

Our investigation of the structure of $[Cu(hfac)_2(NPz^{Et})]\cdot 0.5C_7H_{16}$ showed that the solid phase of this compound is formed by polymer chains with a "head-to-head" motif, resulting from the bridging coordination of NPz^{Et}, with the centrosymmetric coordination of the Cu(II) atom in the $Cu(hfac)_2$ matrixes complemented to octahedral by two N_{Pz} atoms of the pyrazole rings or by two O_{NO} atoms of the nitroxide groups (Figure 2). At 240 K, the $\{CuO_6\}$ units are elongated octahedra with $Cu-O_{NO}$ axial distances of 2.287(3) Å and $Cu-O_{hfac}$ equatorial distances of 1.925(3) and 2.015(3) Å. The coordination polyhedron is similar for $\{CuO_4N_2\}$ units, in which the axial positions are occupied by the N_{Pz} atoms ($d(Cu-N_{Pz})$ = 2.353(4) Å), and the equatorial positions by the O_{hfac} atoms (1.956(3) and 1.982(3) Å).

Studies of the temperature dynamics of the structure of $[Cu(hfac)_2(NPz^{Et})]\cdot 0.5C_7H_{16}$ showed that when the temperature decreased from 240 to 85 K, the bond lengths and angles in the ligands (NPz^{Et} and hfac) changed to a small degree. In the $\{CuO_6\}$ and $\{CuO_4N_2\}$ units at 240−190 K, the axial $Cu-O_{NO}$ distances decreased by 0.078 Å (from 2.287(3) to 2.209(3) Å) (Table 1). Further decrease to 150 K in the temperature caused a drastic shortening of the $Cu-O_{NO}$ bonds from 2.209(3) to 2.032(3) Å, which was accompanied by a simultaneous increase in the $Cu-O_{hfac}$ distances in $\{CuO_6\}$ units from 2.078(3) to 2.288(3) Å along one of the $O_{hfac}-Cu-O_{hfac}$ axes. In Jahn−Teller distorted octahedral $\{CuO_6\}$ units at lowered temperatures, the elongated octahedron axis actually shifted from $O_{NO}-Cu-O_{NO}$ to $O_{hfac}-Cu-O_{hfac}$. In contrast, in $\{CuO_4N_2\}$ units, the Cu−N distances increased from 2.353(4) to 2.392(4) Å in this temperature range. When the crystal was further cooled to 85 K, the $Cu-O_{NO}$ and $Cu-N_{Pz}$ bond lengths decreased because of the thermal compression of the crystal, but much less significantly, by 0.024 and 0.021 Å, respectively. The temperature dynamics of the structure of $[Cu(hfac)_2(NPz^{Et})]\cdot 0.5C_6H_{14}$ is similar to that for $[Cu(hfac)_2(NPz^{Et})]\cdot 0.5C_7H_{16}$ (Table 1). Note that the structural data given in Table 1 for

dx.doi.org/10.1021/ic301149e | Inorg. Chem. 2012, 51, 9385−9394

Table 1. Selected Bond Lengths (Å) and Angles (deg) in Solids $[Cu(hfac)_2(NPz^{Et})]\cdot 0.5C_7H_{16}$ and $[Cu(hfac)_2(NPz^{Et})]\cdot 0.5C_6H_{14}$ at Different Temperatures

	compound											
	$[Cu(hfac)_2(NPz^{Et})]\cdot 0.5C_7H_{16}$						$[Cu(hfac)_2(NPz^{Et})]\cdot 0.5C_6H_{14}$					
T, K	85	105	150	190	240		85	105	150	190	240	
Cu(1)−O(01)	2.007(3)	1.999(3)	2.032(3)	2.209(3)	2.287(3)		1.994(4)	2.001(3)	2.006(4)	2.070(5)	2.273(4)	
Cu(1)−O_{hfac}	1.9246(18), 2.3002(17)	1.922(3), 2.310(3)	1.927(3), 2.288(3)	1.928(3), 2.078(3)	1.925(3), 2.015(3)		1.910(4), 2.309(4)	1.927(3), 2.318(3)	1.929(3), 2.326(4)	1.928(4), 2.209(5)	1.937(4), 2.000(4)	
Cu(2)−N(02)	2.372(4)	2.376(4)	2.392(4)	2.380(4)	2.353(4)		2.392(5)	2.409(4)	2.417(4)	2.395(5)	2.369(5)	
Cu(2)−O_{hfac}	1.9620(18), 1.9667(17)	1.955(3), 1.966(3)	1.962(3), 1.969(3)	1.964(7), 1.976(6)	1.956(3), 1.982(3)		1.952(4), 1.963(5)	1.960(3), 1.976(3)	1.962(4), 1.971(4)	1.950(4), 1.966(4)	1.968(4), 1.982(3)	
O(01)−N(01)	1.300(5)	1.312(4)	1.290(5)	1.290(4)	1.293(4)		1.306(6)	1.305(5)	1.303(5)	1.305(7)	1.306(5)	
N(01)−O(01)−Cu(1)	124.7(2)	125.4(3)	126.1(3)	126.2(3)	126.9(3)		125.0(3)	125.0(3)	125.1(3)	126.3(2)	126.8(3)	

$[Cu(hfac)_2(NPz^{Et})]\cdot 0.5C_7H_{16}$ and $[Cu(hfac)_2(NPz^{Et})]\cdot 0.5C_6H_{14}$ were obtained using the same single crystal. The structural changes in $[Cu(hfac)_2(NPz^{Et})]\cdot 0.5C_7H_{16}$ and $[Cu(hfac)_2(NPz^{Et})]\cdot 0.5C_6H_{14}$ after the lowering of temperature from 240 to 85 K explain the form of the experimental dependence $\mu_{eff}(T)$ (Figure 3a and Supporting Information).

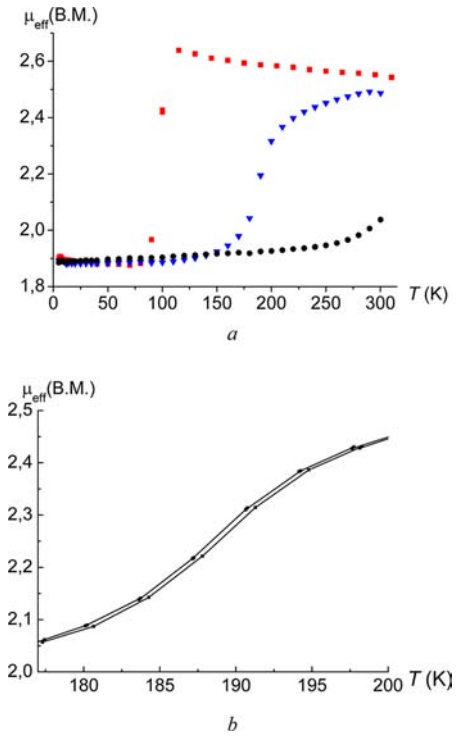

Figure 3. Experimental dependences $\mu_{eff}(T)$ for $[Cu(hfac)_2(NPz^{Me})]$ (red ■), $[Cu(hfac)_2(NPz^{Et})]\cdot 0.5C_7H_{16}$ (blue ▼), and $[Cu(hfac)_2(NPz^{Pr})]$ (●) at 1.0 T (a) and hysteresis for $[Cu(hfac)_2(NPz^{Et})]\cdot 0.5C_7H_{16}$ (b).

The rearrangement of $\{CuO_6\}$ coordination units (three-spin exchange clusters $\{>N\div O-Cu^{2+}-O\div N<\}$) observed at 150–190 K for $[Cu(hfac)_2(NPz^{Et})]\cdot 0.5C_7H_{16}$ and at 180–210 K for $[Cu(hfac)_2(NPz^{Et})]\cdot 0.5C_6H_{14}$ results in a transition of the coordinated nitroxyl O atoms from axial to equatorial positions, which gives rise to strong antiferromagnetic exchange interactions in these compounds[3] and is the reason for the observed decrease in μ_{eff}.

At lowered temperatures ($T \approx 190$ K), the EPR spectra of the polycrystalline sample of $[Cu(hfac)_2(NPz^{Et})]\cdot 0.5C_7H_{16}$ also experienced changes typical of the transition of $\{>N\div O-Cu^{2+}-O\div N<\}$ exchange clusters from weakly to strongly coupled state with a total spin $S = 1/2$.[11] The EPR data point not only to a strong antiferromagnetic exchange ($|J| > 100$ cm^{-1}) in the three-spin clusters at $T < 190$ K, but also to a weak ($J \approx 1$ cm^{-1}) intercluster exchange in the polymer chain between the three-spin clusters of the $\{CuO_6\}$ units and the Cu^{2+} ions of the $\{CuO_4N_2\}$ units.

Because the single crystals of the $[Cu(hfac)_2(NPz^{Me})]\cdot 0.5C_7H_{16}$ and $[Cu(hfac)_2(NPz^{R})]\cdot 0.5C_6H_{14}$ solvates (R = Me, Pr, Bu) easily lose the solvent and decompose under ambient conditions, they were extracted from under the layer of the mother solvent immediately before the XRD experiment and coated with epoxide resin to avoid their decomposition. For the individual $[Cu(hfac)_2(NPz^{Me})]\cdot 0.5C_7H_{16}$ and $[Cu(hfac)_2(NPz^{R})]\cdot 0.5C_6H_{14}$ phases (R = Me, Pr, Bu), however, reliable

dx.doi.org/10.1021/ic301149e | Inorg. Chem. 2012, 51, 9385–9394

magnetochemical data were not obtained because of the insufficient kinetic stability of the solvates.

The structural characteristics of the compounds are presented in Table 2. All hexane solvates and $[Cu(hfac)_2(NPz^{Me})]\cdot 0.5C_7H_{16}$, as well as $[Cu(hfac)_2(NPz^{Et})]\cdot 0.5C_7H_{16}$ (Figure 2), are formed by polymer chains with a "head-to-head" motif. For $[Cu(hfac)_2(NPz^{Me})]\cdot 0.5C_7H_{16}$ at low temperatures (150, 105, and 85 K), the $Cu-O_{NO}$ distances in the $\{CuO_6\}$ units are markedly shortened, although they corresponded to the high-spin state of the $\{>N\div O-Cu^{2+}-O\div N<\}$ clusters over the whole range of measurements. In the $\{CuO_6\}$ units in $[Cu(hfac)_2(NPz^{Pr})]\cdot 0.5C_6H_{14}$, the Cu(1)–O(01) distances at 240 K were noticeably shorter than in $[Cu(hfac)_2(NPz^{Et})]\cdot 0.5C_7H_{16}$ (2.220(3) Å) and shortened to 2.019(2) Å when the temperature was lowered to 85 K (Table 3). In $[(Cu(hfac)_2(NPz^{Bu})]\cdot 0.5C_6H_{14}$, the O_{NO} atoms lie in the equatorial plane of the Cu bipyramid already at 240 K (the distances are $Cu-O_{NO}$ = 2.000(2) Å, $Cu-O_{hfac}$ = 1.930(2) Å) with two O_{hfac} atoms displaced to the axial positions ($Cu-O_{hfac}$ = 2.358(2) Å). If we consider the magnetostructural correlations of $[Cu(hfac)_2(NPz^{Et})]\cdot 0.5C_7H_{16}$ (Table 1), we can conclude that the $Cu-O_{NO}$ distances for $[(Cu(hfac)_2(NPz^{Bu})]\cdot 0.5C_6H_{14}$ (Table 3) correspond to the geometry of the low-spin state of the $\{>N\div O-Cu^{2+}-O\div N<\}$ clusters already at room temperature.

A comparison of the structural characteristics of the pairs $[Cu(hfac)_2(NPz^{Me})]\cdot 0.5C_7H_{16}$–$[Cu(hfac)_2(NPz^{Me})]\cdot 0.5C_6H_{14}$ and $[Cu(hfac)_2(NPz^{Et})]\cdot 0.5C_7H_{16}$–$[Cu(hfac)_2(NPz^{Et})]\cdot 0.5C_6H_{14}$ (Tables 1 and 2) shows that if the R substituent is the same, the replacement of the solvent has little effect on the structural characteristics of the polymer chain. The most significant difference in the structural parameters in the $[Cu(hfac)_2(NPz^{Me})]\cdot 0.5C_7H_{16}$–$[Cu(hfac)_2(NPz^{Me})]\cdot 0.5C_6H_{14}$ pair lies in a drastic shortening of the Cu–N distances in the $\{CuO_4N_2\}$ units at lowered temperatures along with pronounced shortening of the $Cu-O_{NO}$ distances in the $\{CuO_6\}$ units in $[Cu(hfac)_2(NPz^{Me})]\cdot 0.5C_6H_{14}$.

The single crystals of the $[Cu(hfac)_2(NPz^{R})]$ complexes containing no solvate molecules were not obtained. Studies of the magnetic properties and temperature dynamics of the EPR spectra of desolvated $[Cu(hfac)_2(NPz^{R})]$ (R = Me, Pr, Bu), however, indicate that they contain $\{>N\div O-Cu^{2+}-O\div N<\}$ clusters. In the case of $[Cu(hfac)_2(NPz^{Me})]$ at T < 85 K, the spectra show a characteristic change, which points to a drastic strengthening of antiferromagnetic exchange coupling and a transition of three-spin clusters to a state with a total spin S = 1/2.[12] For $[Cu(hfac)_2(NPz^{Pr})]$ at T < 290 K, the EPR spectra have shape similar to the spectra of $[Cu(hfac)_2(NPz^{Me})]$ and $[Cu(hfac)_2(NPz^{Et})]\cdot 0.5C_7H_{16}$ at T < 85 and T < 190 K, respectively; that is, in $[Cu(hfac)_2(NPz^{Pr})]$, strong antiferromagnetic exchange interactions dominate already at 240–300 K.

The temperature dependences of the effective magnetic moment (μ_{eff}) are presented in Figure 3a for the polycrystalline samples of desolvated $[Cu(hfac)_2(NPz^{Me})]$ and $[Cu(hfac)_2(NPz^{Pr})]$ and the solvate $[Cu(hfac)_2(NPz^{Et})]\cdot 0.5C_7H_{16}$ and in the Supporting Information for $[Cu(hfac)_2(NPz^{Et})]\cdot 0.5C_6H_{14}$. For $[Cu(hfac)_2(NPz^{Me})]$, μ_{eff}, which is 2.54 μ_B at 310 K, corresponds to the theoretical spin only value 2.45 μ_B for two noninteracting paramagnetic centers with S = 1/2 at g = 2. When the sample was cooled to 115 K, μ_{eff} gradually increased to 2.64 μ_B, indicating that ferromagnetic exchange interactions dominated in the solid $[Cu(hfac)_2(NPz^{Me})]$. Below 115 K, μ_{eff} drastically decreased to 1.88 μ_B, which is characteristic for systems with one unpaired electron. Thereafter, it

Table 2. Selected Bond Lengths (Å) and Angles (deg) in Solid $[Cu(hfac)_2(NPz^{Me})]\cdot 0.5C_7H_{16}$ and $[Cu(hfac)_2(NPz^{Me})]\cdot 0.5C_6H_{14}$ at Different Temperatures

	compound							
	$[Cu(hfac)_2(NPz^{Me})]\cdot 0.5C_7H_{16}$				$[Cu(hfac)_2(NPz^{Me})]\cdot 0.5C_6H_{14}$			
T, K	85	105	150	240	85	150	240	
Cu(1)–O(01)	2.346(4)	2.350(7)	2.369(2)	2.399(2)	2.362(2)	2.370(2)	2.400(1)	
Cu(1)–O_{hfac}	1.931(3), 1.938(3)	1.924(9), 1.940(10)	1.940(2), 1.943(2)	1.936(2), 1.937(2)	1.940(2), 1.953(2)	1.937(2), 1.949(2)	1.937(1), 1.944(1)	
Cu(2)–N(02)	2.318(4)	2.337(9)	2.331(3)	2.326(2)	2.083(2)	2.209(2)	2.247(2)	
Cu(2)–O_{hfac}	1.963(3), 1.980(3)	1.957(9), 1.977(10)	1.960(2), 1.982(2)	1.964(2), 1.994(2)	1.965(2), 2.218(2)	1.972(2), 2.081(2)	1.970(1), 2.052(1)	
O(01)–N(01)	1.302(6)	1.288(9)	1.304(3)	1.297(2)	1.303(3)	1.301(3)	1.301(2)	
N(01)–O(01)–Cu(1)	130.0(4)	132.0(9)	131.3(2)	134.0(2)	126.5(2)	128.2(2)	132.9(1)	

dx.doi.org/10.1021/ic301149e | Inorg. Chem. 2012, 51, 9385–9394

Table 3. Selected Bond Lengths (Å) and Angles (deg) in Solid $[Cu(hfac)_2(NPz^{Pr})]\cdot 0.5C_6H_{14}$ and $[(Cu(hfac)_2(NPz^{Bu})]\cdot 0.5C_6H_{14}$ at Different Temperatures

	compound			
	$[Cu(hfac)_2(NPz^{Pr})]\cdot 0.5C_6H_{14}$			$[(Cu(hfac)_2NPz^{Bu}]\cdot 0.5C_6H_{14}$
T, K	85	150	240	240
Cu(1)−O(01)	2.019(2)	2.024(3)	2.220(3)	2.000(2)
Cu(1)−O_{hfac}	1.937(2), 2.324(2)	1.934(3), 2.321(3)	1.914(3), 2.075(3)	1.930(2), 2.358(2)
Cu(2)−N(02)	2.389(3)	2.386(4)	2.398(4)	2.392(2)
Cu(2)−O_{hfac}	1.973(2), 1.974(2)	1.968(3), 1.974(2)	1.948(3), 1.967(3)	1.952(2), 1.967(1)
O(01)−N(01)	1.302(4)	1.299(4)	1.297(4)	1.303(2)
N(01)−O(01)−Cu(1)	125.4(2)	125.8(2)	126.5(3)	125.0(1)

did not change down to helium temperatures. For both $[Cu(hfac)_2(NPz^{Et})]\cdot 0.5C_7H_{16}$ and $[Cu(hfac)_2(NPz^{Et})]\cdot 0.5C_6H_{14}$ solvates, μ_{eff} first gradually decreased from 2.49 to 2.35 μ_B at lowered temperatures, then quickly decreased to 1.90 μ_B at 200−180 K, and then changed insignificantly down to 2 K. The drastic $\sqrt{2}$-fold decrease in μ_{eff} recorded experimentally for $[Cu(hfac)_2(NPz^{Me})]$, $[Cu(hfac)_2(NPz^{Et})]\cdot 0.5C_7H_{16}$, and $[Cu(hfac)_2(NPz^{Et})]\cdot 0.5C_6H_{14}$ corresponds to the vanishing of exactly one-half of all spins in the sample.

For $[Cu(hfac)_2(NPz^{Pr})]$, μ_{eff} gradually decreased from 2.04 μ_B at 300 K and formed a plateau ~1.93 μ_B below 260 K. Finally, for $[(Cu(hfac)_2(NPz^{Bu})]$, μ_{eff} remained ~1.91 μ_B over the whole temperature range (Figure 3a). When the heating/cooling cycle was reversed for the same sample and in repeated measurements for complexes obtained in different syntheses, the dependences $\mu_{eff}(T)$ given in Figure 3 were always reproduced. For $[Cu(hfac)_2(NPz^{Et})]\cdot 0.5C_7H_{16}$, a narrow hysteresis loop was recorded (Figure 3b).

Thus, $[Cu(hfac)_2(NPz^{Me})]$, $[Cu(hfac)_2(NPz^{Et})]\cdot 0.5C_7H_{16}$, and $[Cu(hfac)_2(NPz^{Et})]\cdot 0.5C_6H_{14}$, whose $\mu_{eff}(T)$ curves showed magnetic anomalies at 115, 190, and 200 K, respectively, are the first examples of complexes with *N-tert*-butyl-*N*-alkylpyrazolyl-nitroxides, for which spin transitions were recorded. The magnetic anomalies inherent in $[Cu(hfac)_2(NPz^{Me})]$ and $[Cu(hfac)_2(NPz^{Et})]\cdot 0.5C_7H_{16}$ were accompanied by thermochromic effects (Figure 4). Spontaneous heating of the powder samples of

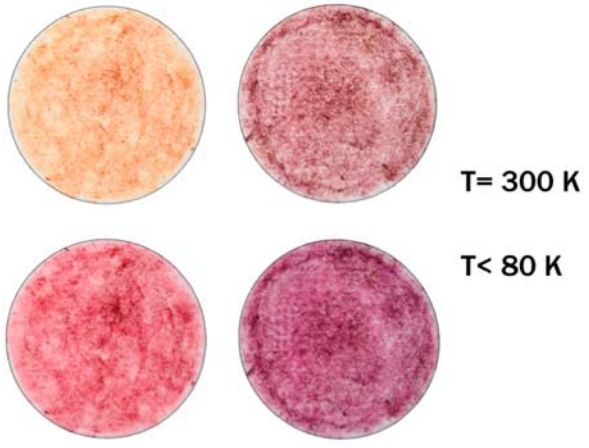

Figure 4. Thermochromism of $[Cu(hfac)_2(NPz^{Me})]$ (left) and $[Cu(hfac)_2(NPz^{Et})]\cdot 0.5C_7H_{16}$ (right).

$[Cu(hfac)_2(NPz^{Me})]$ and $[Cu(hfac)_2(NPz^{Et})]\cdot 0.5C_7H_{16}$ applied to a paper and preliminarily cooled with liquid nitrogen led to a drastic change of color from yellow-brown to brown-red and from brown-violet to dark brown, respectively (the movie in the Supporting Information demonstrates the passage of the thermal front accompanied by a change in the color of the sample).

For $[Cu(hfac)_2(NPz^{Pr})]$ and $[(Cu(hfac)_2(NPz^{Bu})]$ complexes with NPz^R having long alkyl substituents in the pyrazole ring, the temperature of the magnetic anomaly shifted to the range >300 K. For this reason, for $[Cu(hfac)_2(NPz^{Pr})]$, which decomposes above 320 K, it is possible to record only the starting growth of μ_{eff} at T > 270 K. For $[(Cu(hfac)_2(NPz^{Bu})]$, the potential spin transition effect is latent because of its thermal instability at T > 300 K. In the series of compounds under study formed by heterospin chains of the same type in the solid state, the increase in the length of the alkyl substituent R is thus formally accompanied by a pronounced increase in the temperature of the effect.

Our structural and magnetochemical studies of $Cu(hfac)_2$ complexes with nitroxides NPz^R thus revealed a new group of compounds whose heterospin coordination units experienced structural rearrangements accompanied by changes in the magnetic characteristics and color of the samples during variation of temperature.

Complexes with Pivaloylpyrazoles. The driving force for the observed rearrangements in $[Cu(hfac)_2(NPz^R)]$, as well as all compounds of this type studied previously,[3,5−10] was assumed to be the exchange interactions between the unpaired electrons in $\{>N\div O-Cu^{2+}-O\div N<\}$ heterospin clusters; when the nitroxyl groups pass to the equatorial positions, these interactions sharply increase, leading to a decrease in the free energy of the solid. The strong antiferromagnetic exchange interactions that appear in $\{>N\div O-Cu^{2+}-O\div N<\}$ exchange clusters actually serve as a certain increment to the Cu−O bond energy. This exchange and hence increment are impossible for $Cu(hfac)_2$ complexes with diamagnetic structural analogues of nitroxides. This was shown experimentally by comparing the magnetostructural correlations for $Cu(hfac)_2$ complexes with NPz^R and PPz^R. Pivaloylpyrazoles PPz^R synthesized in this study are unique because, while being very close topological analogues of nitroxides NPz^R, they form the same polymers as NPz^R in their reactions with $Cu(hfac)_2$.

The general procedure for the synthesis of PPz^R is given in the Experimental Section. The interaction of $Cu(hfac)_2$ with PPz^R (R = Et, Me, Pr) in heptane led to the formation of $[Cu(hfac)_2(PPz^{Et})]$ and solvates $[Cu(hfac)_2(PPz^{Me})]\cdot 0.5C_7H_{16}$, $[Cu(hfac)_2(PPz^{Pr})]\cdot 0.5C_7H_{16}$. All solids are formed by polymer chains with a "head-to-head" motif similar to those in $[Cu(hfac)_2(NPz^R)]$. Although the $[Cu(hfac)_2(PPz^{Me})]\cdot 0.5C_7H_{16}$ and $[Cu(hfac)_2(PPz^{Pr})]\cdot 0.5C_7H_{16}$ crystals were stable in solution for a long time, they were coated with epoxide resin after their separation from the mother solution before the XRD experiment because they gradually lose the solvent molecules and decompose under ambient conditions. Figure 2b shows a

dx.doi.org/10.1021/ic301149e | *Inorg. Chem.* 2012, 51, 9385−9394

Table 4. Selected Bond Length (Å) and Angles (deg) for $[Cu(hfac)_2(PPz^{Me})]\cdot 0.5C_7H_{16}$, $[Cu(hfac)_2(PPz^{Et})]$, and $[Cu(hfac)_2(PPz^{Pr})]\cdot 0.5C_7H_{16}$ at Different Temperatures

	compound						
	$[Cu(hfac)_2(PPz^{Me})]\cdot 0.5C_7H_{16}$		$[Cu(hfac)_2(PPz^{Et})]$			$[Cu(hfac)_2(PPz^{Pr})]\cdot 0.5C_7H_{16}$	
T, K	85	240	100	150	240	85	240
Cu(1)−O(01)	2.409(3)	2.417(2)	2.335(1)	2.342(1)	2.355(2)	2.358(1)	2.368(2)
Cu(2)−N(02)	2.262(4)	2.349(3)	2.410(1)	2.418(1)	2.439(2)	2.394(2)	2.410(2)
O(01)−C(01)	1.251(5)	1.236(3)	1.229(1)	1.222(2)	1.219(3)	1.233(2)	1.221(3)
C(01)−O(01)−Cu(1)	144.4(4)	145.9(2)	133.39(8)	135.2(1)	138.2(2)	129.8(1)	137.2(2)

fragment of the $[Cu(hfac)_2(PPz^{Et})]$ polymer chain. The same structure is typical for chains in $[Cu(hfac)_2(PPz^{Me})]\cdot 0.5C_7H_{16}$ and $[Cu(hfac)_2(PPz^{Pr})]\cdot 0.5C_7H_{16}$ crystals (Supporting Information). A comparison of the structures of chains in $Cu(hfac)_2$ complexes with nitroxides NPz^R and pivaloylpyrazoles PPz^R showed that they are very similar (Figure 2).

An XRD study of $[Cu(hfac)_2(PPz^{Et})]$ in the range 240−85 K did not reveal any structural changes except for a small monotonic shortening of distances. The $[Cu(hfac)_2(PPz^{Pr})]\cdot 0.5C_7H_{16}$ solvate behaved similarly in this temperature range. In the structure of $[Cu(hfac)_2(PPz^{Me})]\cdot 0.5C_7H_{16}$, the Cu−N distances in the $\{CuO_4N_2\}$ units shortened on cooling (Table 4). The magnetic moments for $Cu(hfac)_2$ complexes with PPz^R have practically no changes in the temperature range 2−300 K and were due only to the contribution from the Cu^{2+} ions.

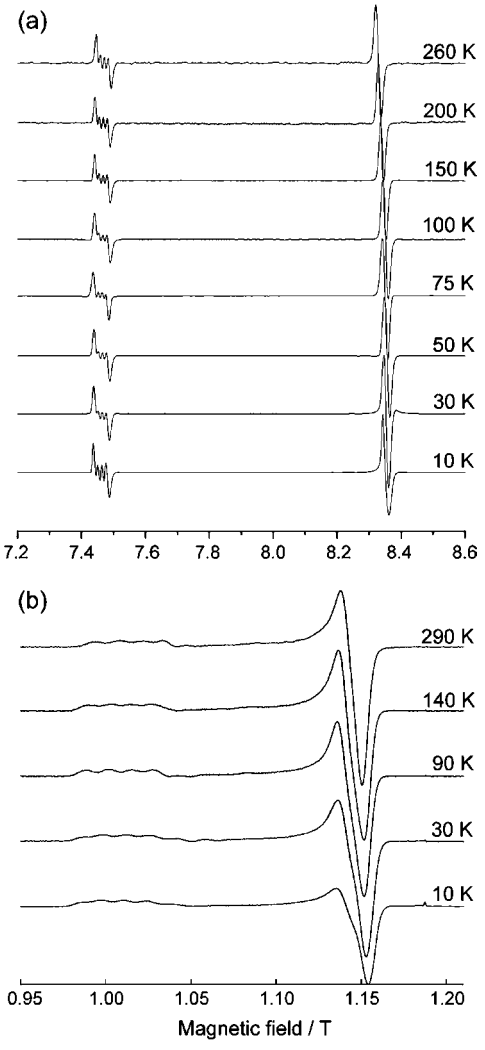

Figure 5. (a) 244 GHz single-crystal EPR spectra of $[Cu(hfac)_2(PPz^{Et})]$ at T = 10−260 K ($\nu_{mw} \approx$ 243.68 GHz, arbitrary crystal orientation). (b) Q-band powder EPR spectra of $[Cu(hfac)_2(PPz^{Et})]$ at T = 10−290 K ($\nu_{mw} \approx$ 33.21 GHz). The temperature values are given on the right.

It is realistic to expect that structural rearrangements (if any) can be detected using EPR. If the elongated Jahn−Teller axis of the six-coordinated copper(II) ion is flipped, the largest component of the g tensor (g_z) must also interchange with one of the other two components (g_x or g_y) that can be observed in the EPR spectrum of the single crystal. To enhance the spectral resolution, we used high-field EPR at 244 GHz. Figure 5a shows the single-crystal EPR spectra of $[Cu(hfac)_2(PPz^{Et})]$ measured at 244 GHz in the temperature range 10−260 K. The spectra exhibit negligible changes with temperature, which cannot be associated with the Jahn−Teller axis flip. The Q-band powder EPR spectra (Figure 5b) also did not change noticeably with temperature. For $[Cu(hfac)_2(PPz^{Me})]\cdot 0.5C_7H_{16}$ and $[Cu(hfac)_2(PPz^{Pr})]\cdot 0.5C_7H_{16}$, we also could not observe any manifestations of abrupt structural rearrangements (Supporting Information).

CONCLUSIONS

A new family of heterospin polymer chain complexes of $Cu(hfac)_2$ with 1-*R*-4-(*N*-*tert*-butyl-*N*-oxylamino)-pyrazoles NPz^R was synthesized. During the repeated cooling−heating cycles, the solid complexes experienced reversible structural rearrangements accompanied by abrupt changes in the effective magnetic moment. Synthetic procedures were developed for the diamagnetic analogues of NPz^R, 2,2-dimethyl-1-(1-*R*-1*H*-pyrazol-4-yl)propan-1-ones PPz^R containing a >C═O group instead of the paramagnetic >N÷O group, and for $[Cu(hfac)_2(PPz^R)]$ polymer chain complexes having the same structure as $[Cu(hfac)_2(NPz^R)]$. A comparative analysis of the temperature dynamics of the structure and magnetic characteristics of $[Cu(hfac)_2(NPz^R)]$ and $[Cu(hfac)_2(PPz^R)]$ provided experimental evidence that the presence of a coordinated nitroxyl fragment in a solid heterospin compound is an essential condition for the breathing crystal effect. The coordination of the O÷*N*< fragment by the Cu(II) ion provides the potential for considerable displacements of atoms in solid $Cu(hfac)_2$ complexes with nitroxides, favored by the appearance of strong antiferromagnetic interactions in $\{>N\div O-Cu^{2+}-O\div N<\}$ exchange clusters. The absence of such interactions in $[Cu(hfac)_2(PPz^R)]$ crystals leads to a negligible dependence of $\{CuO_6\}$ coordination units geometry on temperature despite the similarity of the spatial structures of NPz^R and PPz^R.

EXPERIMENTAL SECTION

General Procedures. 1-Methyl, 1-ethyl-, and 1-propyl-4-bromo-1*H*-pyrazoles[12] were synthesized by bromination of the corresponding 1-alkylpyrazoles with NBS in CCl_4 and distilled in vacuum. 1-Methyl-,

dx.doi.org/10.1021/ic301149e | Inorg. Chem. 2012, 51, 9385−9394

1-ethyl-, and 1-propyl-1*H*-pyrazol-4-carbaldehydes were prepared from the corresponding 1-alkylpyrazoles[13] by the Vilsmeier reaction. $Cu(hfac)_2$[14] was sublimed before use. Tetrahydrofuran (THF) was fresh distilled over sodium hydride. Other chemicals of the highest purity available were purchased from Acros and Aldrich and used as received. The reactions were monitored by TLC using silica gel 60 F_{254} aluminum sheets, Merck. Chromatography was carried out with the use of Merck 0.063−0.100 mm silica gel for column chromatography. C, H, and N elemental analyses were carried out on a CHN analyzers EA-3000 and Carlo Erba 1106 in the Chemical Analytical Center of the Novosibirsk Institute of Organic Chemistry. The melting points were determined on an SMP3 Stuart melting point apparatus. Infrared spectra (4000−400 cm^{-1}) were recorded with a Bruker VECTOR 22 instrument in KBr pellets. ^1H and ^{13}C NMR spectra were recorded at 25 °C using a Bruker Avance 400 spectrometer locked to the deuterium resonance of the solvent; the chemical shifts are reported in parts per million (ppm), and the solvent was used as internal standard. HRMS were recorded on a DFS instrument using the electron impact ionization technique (70 eV). X-Band CW EPR spectra of the nitroxides were recorded in dilute degassed toluene solutions at room temperature on a Bruker EMX spectrometer at MW power 2 mW, modulation amplitude 0.01 mT at 100 kHz, single scan of 4096 points at 1310 ms per point, time constant 1310 ms, and modeled with Winsim v.0.96 free package as described earlier;[15] the isotropic *g*-values were determined using solid DPPH as standard, and the accuracy of the hyperfine coupling constants and *g*-values was 0.005 mT and 0.0001, respectively. Q-Band EPR measurements were performed using a Bruker Elexsys E580 spectrometer equipped with an Oxford Instruments temperature control system using a ER 5106QT resonator. A high-field EPR spectrometer[16] equipped with an ICE-Oxford cryogenic system was used for experiments at 244 GHz. These high-field EPR experiments were carried out without a resonator using induction mode detection. The magnetic susceptibility of the polycrystalline complexes was measured with a Quantum Design MPMSXL SQUID magnetometer in the temperature range 2−300 K with magnetic fields of up to 5 kOe. None of the complexes exhibited any field dependence of molar susceptibility at low temperatures. The diamagnetic corrections were applied using the Pascal constants. The effective magnetic moment was calculated as $\mu_{eff}(T) = [(3k/N_A\mu_B^2)\chi'_M T]^{1/2} \approx (8\chi'_M T)^{1/2}$, where χ'_M is the corrected molar susceptibility.

Syntheses of NPz^R and PPz^R.

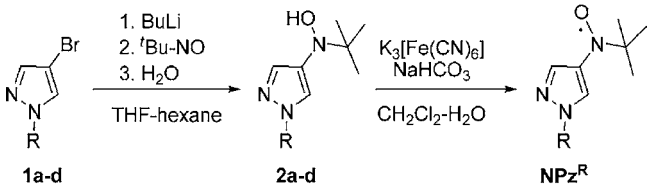

1a-d **2a-d** **NPz^R**

R = Me (**a**), Et (**b**), Pr (**c**), Bu (**d**)

*N-tert-Butyl-N-(1-methyl-1H-pyrazol-4-yl)hydroxylamine (**2a**).* A 2.5 M solution of BuLi in hexane (5.47 mL, 12.7 mmol) was added dropwise to the solution of 4-bromo-1-methyl-1*H*-pyrazole (**1a**) (2.0 g, 12.4 mmol) in absolute THF (20 mL) vigorously stirred under argon at −90 °C. The reaction mixture was stirred for 30 min, and a solution of 2-methyl-2-nitrosopropane (1.08 g, 12.4 mmol) in THF (10 mL) was added to it. After 1 h, the cooling was stopped and the reaction mixture was allowed to warm to room temperature. Water (15 mL) and CH_2Cl_2 (30 mL) were added to the resulting mixture. The organic phase was separated, and the aqueous phase was extracted with CH_2Cl_2 (5 × 20 mL). The extract and the organic layer were combined, then dried over anhydrous Na_2SO_4, filtered through the Al_2O_3 layer, and concentrated under reduced pressure. The residue was crystallized by storing it under a heptane layer at −15 °C for 12 h. The product was filtered off and recrystallized from a mixture of ethyl acetate with heptane. Yield 0.66 g (31%); colorless needle crystals; mp 101−102 °C. IR: ν = 3211, 3139, 3086, 2982, 2933, 2868, 1681, 1556, 1460, 1441, 1418, 1387, 1360, 1348, 1320, 1210, 1168, 1115, 1073, 1041, 1017, 996, 949, 928, 886, 852, 790, 706, 685, 646, 634, 561, 496, 434 cm^{-1}. ^1H NMR (400 MHz, $CDCl_3$): δ = 1.10 (s, 9H, ^{t}Bu), 3.81 (s, 3H, *N*−Me), 7.17 and 7.29 (both s, 1H each, *C*(3)−H, *C*(5)−H). ^{13}C NMR (100 MHz, $CDCl_3$): δ = 25.4 ($C(\underline{C}H_3)_3$), 39.1 (Me), 59.9 ($\underline{C}(CH_3)_3$), 124.7 and 134.7 (C(3), C(5)), 133.3 (C(4)). Anal. Calcd for $C_8H_{15}N_3O$: C, 56.8; H, 8.9; N, 24.8. Found: C, 57.0; H, 8.9; N, 25.0.

*N-tert-Butyl-N-(1-R-1H-pyrazol-4-yl)hydroxylamines (**2b−d**).* These were obtained from corresponding 4-bromo-1-*R*-1*H*-pyrazoles (**1b−d**) by a procedure similar to the one used for the synthesis of **2a** (Supporting Information).

4-(N-tert-Butyl-N-oxylamino)-1-methyl-1H-pyrazole (NPz^{Me}). $K_3[Fe(CN)_6]$ (89 mg, 0.27 mmol) was added to a stirred mixture of hydroxylamine **2a** (30 mg, 0.18 mmol), $NaHCO_3$ (30 mg, 0.4 mmol), CH_2Cl_2 (5 mL), and H_2O (2 mL). The reaction mixture was stirred at room temperature for 1 h. The bright orange organic phase was separated, dried over anhydrous Na_2SO_4, and filtered. The filtrate was diluted with heptane (10 mL). The resulting solution was evaporated at reduced pressure and a bath temperature of ∼35 °C. The residue was dissolved in heptane (5 mL). The solution was filtered and evaporated. The product was red oil. HRMS, *m*/*z*: 168.1124 (M^+, calcd for $C_8H_{14}N_3O$ 168.1137). MS, *m*/*z* (%): 168 (M^+, 5), 167 (21), 153 (19), 138 (61), 122 (17), 113 (14), 112 (59), 111 (9), 97 (14), 96 (20), 82 (11), 70 (30), 69 (10), 57 (100). EPR: g_{iso} = 2.0055; $A_{>N-O}(1N)$ = 1.269 mT, $A_{N(2)}(1N)$ = 0.032 mT, $A_{N(1)}(1N)$ = 0.018 mT, $A_{C(5)-H}(1H)$ = 0.254 mT, $A_{C(3)-H}(1H)$ = 0.155 mT, $A_{N-Me}(3H)$ = 0.065 mT.

4-(N-tert-Butyl-N-oxylamino)-1-R-1H-pyrazoles (NPz^R). These were obtained from corresponding *N-tert*-Butyl-*N*-(1-*R*-1*H*-pyrazol-4-yl)-hydroxylamines (**2b−d**) by a procedure similar to the one used for the synthesis of NPz^{Me} (Supporting Information).

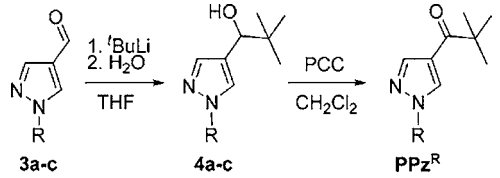

3a-c **4a-c** **PPz^R**

R = Me (**a**), Et (**b**), Pr (**c**)

*1-(1-Ethyl-1H-pyrazol-4-yl)-2,2-dimethylpropan-1-ol (**4b**).* A 1.7 M solution of ^{t}BuLi in pentane (8 mL, 13.6 mmol) was added dropwise to the vigorously stirred solution of 1-ethyl-1*H*-pyrazole-4-carbaldehyde (**3b**) (1.5 g, 12.1 mmol) in THF (25 mL) at −80 °C under argon. The cooling was stopped. The reaction mixture was allowed to warm to room temperature and then diluted with water (70 mL). The product was extracted with CH_2Cl_2 (5 × 30 mL); the combined extracts were dried over anhydrous Na_2SO_4 and concentrated under reduced pressure. The residue was recrystallized from a hexane−ethyl acetate (5: 1) mixture. The pale yellow crystalline precipitate was filtered off. Yield 0.82 g (37%); mp 79−82 °C. IR: ν = 3316, 2952, 2906, 2868, 1724, 1681, 1632, 1559, 1478, 1465, 1440, 1406, 1379, 1360, 1296, 1243, 1177, 1159, 1103, 1059, 1010, 960, 901, 864, 818, 788, 767 cm^{-1}. ^1H NMR (300 MHz, $CDCl_3$): δ = 0.81 (s, 9 H, ^{t}Bu), 1.29 (t, *J* = 7.3 Hz, 3 H, CH_3), 4.07 (q, *J* = 7.3 Hz, 2 H, *N*−CH_2), 4.16 and 4.86 (both d, *J* = 4.4 Hz, 1 H each, C$\underline{H}$−OH, CH−O$\underline{H}$), 7.24 (s, 1 H, *C*(3)−H), 7.49 (s, 1 H, *C*(5)−H). HRMS, *m*/*z*: 182.1415 (M^+, calcd for $C_{10}H_{18}N_2O$ 182.1419). MS, *m*/*z* (%): 182 (M^+, 1), 167 (4), 126 (5), 125 (100), 123 (2), 97 (3), 95 (1), 69 (5), 57 (1), 42 (1).

*2,2-Dimethyl-1-(1-R-1H-pyrazol-4-yl)propan-1-ols (**4a** and **4c**).* These were obtained by a procedure similar to the one used for the synthesis of **4b** (Supporting Information).

2,2-Dimethyl-1-(1-ethyl-1H-pyrazol-4-yl)propan-1-one (PPz^{Et}). PCC (0.49 g, 2.25 mmol) was added to a stirred solution of **4b** (0.25 g, 1.4 mmol) in CH_2Cl_2 (20 mL). The reaction mixture was stirred at room temperature for 1.5 h, diluted with diethyl ether (20 mL), again stirred for 10 min, and filtered through a silica gel layer (1 × 20 cm, diethyl ether as eluent). The filtrate was concentrated in a vacuum, and a pale yellow oil of PPz^{Et} was obtained. Yield 0.13 g (53%); R_f = 0.80 (SiO_2, ethyl acetate). IR: ν = 3269, 3130, 2976, 2871, 1654, 1540, 1477, 1392, 1264, 1238, 1168, 1112, 1080, 1052, 988, 956,

dx.doi.org/10.1021/ic301149e | *Inorg. Chem.* 2012, 51, 9385−9394

922, 897, 870, 810, 766 cm^{-1}. ^1H NMR (300 MHz, $CDCl_3$): δ = 1.29 (s, 9H, ^tBu), 1.49 (t, J = 7.3 Hz, 3H, CH_3), 4.16 (q, J = 7.3 Hz, 2H, $N-CH_2$), 7.90 and 7.92 (both s, 1H each, $C(3)-H$, $C(5)-H$). HRMS, m/z: 180.1258 (M^+, calcd for $C_{10}H_{16}N_2O$ 180.1263). MS, m/z (%): 180 (M^+, 3), 139 (2), 137 (1), 125 (1), 124 (5), 123 (100), 95 (18), 68 (1), 57 (2), 41 (2), 39 (1), 29 (1), 28 (2), 18 (2).

2,2-Dimethyl-1-(1-R-1H-pyrazol-4-yl)propan-1-ones (PPz^{Me} and PPz^{Pr}). These were obtained by a procedure similar to the one used for the synthesis of PPz^{Et}.

[Cu(hfac)$_2$(NPz^{Me})]. A solution of nitroxide NPz^{Me} in heptane (10 mL) obtained from **2a** (30 mg, 0.16 mmol) was added to the solution of $Cu(hfac)_2$ (74 mg, 0.16 mmol) in heptane (5 mL) and stored for 12 h at −15 °C. The crystalline precipitate was filtered off, washed with cold heptane, and dried in air for 10 min. The product was stored in a refrigerator at −15 °C. Yield 90 mg (71%); yellow brown crystals. Anal. Calcd for $C_{18}H_{16}CuF_{12}N_3O_5$: C, 33.5; H, 2.5; N, 6.5; F, 35.3. Found: C, 33.2; H, 2.7; N, 6.1; F, 33.3.

[Cu(hfac)$_2$(NPz^{Et})]·0.5C$_7$H$_{16}$ and [Cu(hfac)$_2$(NPz^{Et})]·0.5C$_6$H$_{14}$. These were obtained from heptane and hexane, respectively, by a procedure similar to the one used for the synthesis of $[Cu(hfac)_2(NPz^{Me})]$. The yield of $[Cu(hfac)_2(NPz^{Et})]\cdot0.5C_7H_{16}$ was 83 mg (71%); dark violet crystals with a brown tint. Anal. Calcd for $C_{19}H_{18}CuF_{12}N_3O_5\cdot0.5C_7H_{16}$: C, 38.0; H, 3.7; N, 5.9; F, 32.1. Found: C, 37.9; H, 3.4; N, 6.3; F, 32.3. The yield of $[Cu(hfac)_2(NPz^{Et})]\cdot0.5C_6H_{14}$ was 77 mg (66%); dark violet crystals with a brown tint. Anal. Calcd for $C_{19}H_{18}CuF_{12}N_3O_5\cdot0.2C_6H_{14}$: C, 35.8; H, 3.1; N, 6.2; F, 33.7. Found: C, 35.5; H, 3.1; N, 6.2; F, 33.6.

[Cu(hfac)$_2$(NPz^{Pr})]. This was obtained by a procedure similar to the one used for the synthesis of $[Cu(hfac)_2(NPz^{Me})]$ except that hexane solutions of $Cu(hfac)_2$ and NPz^{Pr} (5 mL) were used. The product was dried in air. Yield 74 mg (70%); dark violet crystals with a brown tint. Anal. Calcd for $C_{20}H_{20}CuF_{12}N_3O_5$: C, 35.6; H, 3.0; N, 6.2; F, 33.8. Found: C, 35.2; H, 3.2; N, 5.9; F, 33.4. When the procedure was performed in heptane, the finely crystalline $[Cu(hfac)_2(NPz^{Pr})]$ product always contained greenish brown crystals of two modifications of the $[(Cu(hfac)_2)_3(NPz^{Pr})_2]$ complex.

[(Cu(hfac)$_2$)$_3$(NPz^{Bu})$_2$)]. This was obtained by a procedure similar to the one used for the synthesis of $[Cu(hfac)_2(NPz^{Pr})]$. Yield 50 mg (20%); violet-brown crystals. Anal. Calcd for $C_{21}H_{22}CuF_{12}N_3O_5$: C, 36.7; H, 3.2; N, 6.1; F, 33.1. Found: C, 36.2; H, 3.0; N, 6.1; F, 33.4. When the procedure was performed in heptane, the main product $[(Cu(hfac)_2(NPz^{Bu})]$ contained perfect crystals of $[(Cu(hfac)_2)_3(NPz^{Bu})_2]$.

[Cu(hfac)$_2$(PPz^{Et})]. A mixture of $Cu(hfac)_2$ (0.38 g, 0.79 mmol) and PPz^{Et} (0.13 g, 0.72 mmol) was dissolved in heptane (17 mL) at 50 °C. The resulting dark green solution was slowly cooled to room temperature. After 20 h, the resulting green needle crystals were filtered off. Yield 0.27 g (57%); mp 120−125 °C. IR: ν = 3149, 2985, 2352, 1643, 1603, 1559, 1533, 1486, 1399, 1354, 1261, 1227, 1146, 1106, 1006, 967, 923, 880, 768, 745 cm^{-1}. Anal. Calcd for $C_{20}H_{18}CuF_{12}N_2O_5$: C, 36.5; H, 2.8; N, 4.3. Found: C, 36.9; H, 2.7; N, 3.9.

[Cu(hfac)$_2$(PPz^{Me})]. This was obtained by a procedure similar to the one used for the synthesis of $[Cu(hfac)_2(PPz^{Et})]$. Yield 0.42 g (44%). IR: ν = 3142, 2977, 1643, 1559, 1536, 1487, 1399, 1354, 1261, 1225, 1145, 1106, 994, 923, 881, 801, 768, 746 cm^{-1}. Anal. Calcd for $C_{19}H_{16}CuF_{12}N_2O_5$: C, 35.4; H, 2.5; N, 4.4. Found: C, 35.6; H, 2.5; N, 4.2.

[Cu(hfac)$_2$(PPz^{Pr})]. This was obtained by a procedure similar to the one used for the synthesis of $[Cu(hfac)_2(PPz^{Et})]$. Yield 0.09 g (27%). IR: ν = 3444, 3137, 2980, 2911, 2885, 1646, 1597, 1559, 1538, 1489, 1463, 1400, 1368, 1353, 1263, 1219, 1145, 1107, 1040, 1004, 923, 883, 815, 798, 766, 745 cm^{-1}. Anal. Calcd for $C_{21}H_{20}CuF_{12}N_2O_5$: C, 37.5; H, 3.0; N, 4.2. Found: C, 37.1; H, 3.0; N, 4.2.

X-ray Crystallography. Crystals for an XRD analysis were selected directly from solution and immediately coated with a layer of epoxide resin. The intensity data for the single crystals were collected by the standard procedure on SMART APEX II CCD and SMART APEX II DUO (Bruker AXS) automated diffractometers (Mo Kα radiation, graphite monochromator). The structures were solved by direct methods and refined by the full-matrix least-squares procedure anisotropically for non-hydrogen atoms. The H atoms were partially located in difference electron density syntheses, and the other atoms were calculated geometrically and included as riding groups in the refinement. All calculations were fulfilled with the SHELXTL 6.14 program package. Imperfection and the small size of crystals in some cases led to a small amount of independent reflections with $I > 2\sigma_I$ in experimental data despite the substantial increase in scan time to 60 s per frame. Crystallographic data and experimental details for compounds under discussion are given in the Supporting Information.

■ ASSOCIATED CONTENT

Ⓢ Supporting Information

Synthetic procedures; crystallographic data for all compounds (in CIF form); EPR spectra for NPz^{Et}, NPz^{Pr}, NPz^{Bu}, $[Cu(hfac)_2(PPz^{Me})]\cdot0.5C_7H_{16}$, and $[Cu(hfac)_2(PPz^{Pr})]\cdot0.5C_7H_{16}$; dependences $\mu_{eff}(T)$ for $[Cu(hfac)_2(NPz^{Et})]\cdot0.5C_6H_{14}$, $[Cu(hfac)_2(PPz^{Me})]\cdot0.5C_7H_{16}$, $[Cu(hfac)_2(PPz^{Et})]$, and $[Cu(hfac)_2(PPz^{Pr})]$; the results of DFT calculations for NPz^{Et} and L^{Et}; and the movie that demonstrates the passage of the thermal front of the phase transition in $[Cu(hfac)_2(NPz^{Me})]$ and $[Cu(hfac)_2(NPz^{Et})]\cdot0.5C_7H_{16}$. This material is available free of charge via the Internet at http://pubs.acs.org.

■ AUTHOR INFORMATION

Corresponding Author

*E-mail: victor.ovcharenko@tomo.nsc.ru.

Notes

The authors declare no competing financial interest.

■ ACKNOWLEDGMENTS

This study was financially supported by the Russian Foundation for Basic Research (grant nos. 11-03-00158, 11-03-00027, 11-03-12001, 12-03-00067, 12-03-31184, and 12-03-31289), RF President grants (MK-4268.2010.3, MK-868.2011.3, MK-6497.2012.3, and MK-1662.2012.3), the Russian Academy of Sciences, and the Siberian Branch of the Russian Academy of Sciences. We are grateful to Prof. Yuri N. Molin for initiating us to look at this problem and Dr. Alex I. Kruppa for help in modeling the EPR spectra.

■ REFERENCES

(1) (a) Eaton, S. S.; Eaton, G. R. *Coord. Chem. Rev.* **1978**, *26*, 207−262. (b) Eaton, S. S.; Eaton, G. R. *Coord. Chem. Rev.* **1988**, *83*, 29−72. (c) Drago, R. S. *Coord. Chem. Rev.* **1980**, *32*, 97−110. (d) Caneschi, A.; Gatteschi, D.; Rey, P. *Prog. Inorg. Chem.* **1991**, *39*, 331−429. (e) Volodarsky, L. B.; Reznikov, V. A.; Ovcharenko, V. I. *Synthetic Chemistry of Stable Nitroxides*; CRC Press, Inc.: Boca Raton, FL, 1994. (f) Iwamura, H.; Inoue, K.; Hayamizu, T. *Pure Appl. Chem.* **1996**, *68*, 243−252. (g) Ovcharenko, V. I.; Maryunina, K. Yu.; Fokin, S. V.; Tretyakov, E. V.; Romanenko, G. V.; Ikorskii, V. N. *Rus. Chem. Bull.* **2004**, *53*, 2406−2427. (h) Luneau, D.; Rey, P. *Coord. Chem. Rev.* **2005**, *249*, 2591−2611. (i) Luneau, D.; Borta, A.; Chumakov, Y.; Jacquot, J.-F.; Jeanneau, E.; Lescop, C.; Rey, P. *Inorg. Chim. Acta* **2008**, *361*, 3669−3676. (j) Caneschi, A.; Gatteschi, D.; Sessoli, R.; Rey, P. *Acc. Chem. Res.* **1989**, *22*, 392−398. (k) Iwamura, H.; Inoue, K. In *Magnetism: Molecules to Materials II. Molecule-Based Materials*; Miller, J. S., Drillon, M., Eds.; Wiley−VCH: Weinheim, 2001; pp 61−108. (l) Oshio, H.; Ito, T. *Coord. Chem. Rev.* **2000**, *198*, 329. (m) Ovcharenko, V. In *Stable Radicals: Fundamentals and Applied Aspects of Odd-Electron Compounds*; Hicks, R. G., Ed.; John Wiley & Sons, Ltd.: Wiltshire, 2010; pp 461−506.

(2) (a) Kahn, O. *Molecular Magnetism*; VCH: New York, 1993. (b) Carlin, R. L. *Magnetochemistry*; Springer-Verlag: Berlin, 1986.

(3) (a) Caneschi, A.; Chiesi, P.; David, L.; Ferraro, F.; Gatteschi, D.; Sessoli, R. *Inorg. Chem.* **1993**, *32*, 1445−1453. (b) Lanfranc de Panthou, F.; Belorizky, E.; Calemczuk, R.; Luneau, D.; Marcenat, C.; Ressouche, E.; Turek, P.; Rey, P. *J. Am. Chem. Soc.* **1995**, *117*, 11247−11253.

(c) Lanfranc de Panthou, F.; Luneau, D.; Musin, R.; Öhrström, L.; Grand, A.; Turek, P.; Rey, P. *Inorg. Chem.* **1996**, *35*, 3484−3491. (d) Iwahory, F.; Inoue, K.; Iwamura, H. *Mol. Cryst. Liq. Cryst.* **1999**, *334*, 533−538. (e) Rey, P.; Ovcharenko, V. I. In *Magnetism: Molecules to Materials II. Molecule-Based Materials*; Miller, J. S., Drillon, M., Eds.; Wiley−VCH: Weinheim, 2003; pp 41−63. (f) Fokin, S.; Ovcharenko, V.; Romanenko, G.; Ikorskii, V. *Inorg. Chem.* **2004**, *43*, 969−977. (g) Baskett, M.; Lahti, P. M.; Paduan-Filho, A.; Oliveira, N. F. *Inorg. Chem.* **2005**, *44*, 6725−6735. (h) Ovcharenko, V. I.; Romanenko, G. V.; Maryunina, K. Yu.; Bogomyakov, A. S.; Gorelik, E. V. *Inorg. Chem.* **2008**, *47*, 9537−9552. (i) Maryunina, K.; Fokin, S.; Ovcharenko, V.; Romanenko, G.; Ikorskii, V. *Polyhedron* **2005**, *24*, 2094−2101. (j) Okazawa, A.; Hashizume, D.; Ishida, T. *J. Am. Chem. Soc.* **2010**, *132*, 11516−11524.

(4) Lim, Y. Y.; Drago, R. S. *Inorg. Chem.* **1972**, *11*, 1334−1338.

(5) (a) Ovcharenko, V. I.; Fokin, S. V.; Romanenko, G. V.; Ikorskii, V. N.; Tretyakov, E. V.; Vasilevsky, S. F. *J. Struct. Chem.* **2002**, *43*, 153−169. (b) Ovcharenko, V. I.; Fokin, S. V.; Romanenko, G. V.; Ikorskii, V. N.; Tretyakov, E. V.; Vasilevsky, S. F.; Sagdeev, R. Z. *Mol. Phys.* **2002**, *100*, 1107−1115. (c) Ovcharenko, V. I.; Maryunina, K. Yu.; Fokin, S. V.; Tretyakov, E. V.; Romanenko, G. V.; Ikorskii, V. N. *Russ. Chem. Bull. (Engl. Transl.)* **2004**, *53*, 2406−2427. (d) Romanenko, G. V.; Maryunina, K. Yu.; Bogomyakov, A. S.; Sagdeev, R. Z.; Ovcharenko, V. I. *Inorg. Chem.* **2011**, *50*, 6597−6609.

(6) (a) Zueva, E. M.; Ryabykh, E. R.; Kuznetsov, An. M. *Russ. Chem. Bull. (Engl. Transl.)* **2009**, *8*, 1654−1662. (b) Postnikov, A. V.; Galakhov, A. V.; Blügel, S. *Phase Transitions* **2005**, *78*, 689−699. (c) Vancoillie, S.; Rulíšek, L.; Neese, F.; Pierloot, K. *J. Phys. Chem. A* **2009**, *113*, 6149−6157.

(7) (a) Morozov, V. A.; Lukzen, N. N.; Ovcharenko, V. I. *J. Phys. Chem. B* **2008**, *112*, 1890−1893. (b) Morozov, V. A.; Lukzen, N. N.; Ovcharenko, V. I. *Russ. Chem. Bull. (Engl. Transl.)* **2008**, *4*, 863−867. (c) Morozov, V. A.; Lukzen, N. N.; Ovcharenko, V. I. *Dokl. Phys. Chem.* **2010**, *430*, 33−35.

(8) (a) Fedin, M.; Veber, S.; Gromov, I.; Ovcharenko, V.; Sagdeev, R.; Schweiger, A.; Bagryanskaya, E. *J. Phys. Chem. A* **2006**, *110*, 2315−2317. (b) Fedin, M.; Veber, S.; Gromov, I.; Ovcharenko, V.; Sagdeev, R.; Bagryanskaya, E. *J. Phys. Chem. A* **2007**, *111*, 4449−4455. (c) Fedin, M.; Veber, S.; Gromov, I.; Maryunina, K.; Fokin, S.; Romanenko, G.; Sagdeev, R.; Ovcharenko, V.; Bagryanskaya, E. *Inorg. Chem.* **2007**, *46*, 11405−11415. (d) Veber, S. L.; Fedin, M. V.; Potapov, A. I.; Maryunina, K. Yu.; Romanenko, G. V.; Sagdeev, R. Z.; Ovcharenko, V. I.; Goldfarb, D.; Bagryanskaya, E. G. *J. Am. Chem. Soc.* **2008**, *130*, 2444−2445. (e) Veber, S. L.; Fedin, M. V.; Romanenko, G. V.; Sagdeev, R. Z.; Bagryanskaya, E. G.; Ovcharenko, V. I. *Inorg. Chim. Acta* **2008**, *361*, 4148−4152. (f) Fedin, M.; Ovcharenko, V.; Bagryanskaya, E. G. In *The Treasures of Eureka, I: Electron Paramagnetic Resonance: From Fundamental Research to Pioneering Applications & Zavoisky Award*; Salikhov, K. M., Ed.; AXAS Publishing Ltd.: Wellington, New Zealand, 2009; pp 122−123. (g) Fedin, M. V.; Veber, S. L.; Sagdeev, R. Z.; Ovcharenko, V. I.; Bagryanskaya, E. G. *Russ. Chem. Bull. (Engl. Transl.)* **2010**, *59*, 1065−1079.

(9) Fedin, M. V.; Veber, S. L.; Maryunina, K. Yu.; Romanenko, G. V.; Suturina, E. A.; Gritsan, N. P.; Sagdeev, R. Z.; Ovcharenko, V. I.; Bagryanskaya, E. G. *J. Am. Chem. Soc.* **2010**, *132*, 13886−13891.

(10) Fedin, M.; Ovcharenko, V.; Sagdeev, R.; Reijerse, E.; Lubitz, W.; Bagryanskaya, E. G. *Angew. Chem., Int. Ed.* **2008**, *47*, 6897−6899.

(11) Fedin, M. V.; Drozdyuk, I. Yu.; Tretyakov, E. V.; Tolstikov, S. E.; Ovcharenko, V. I.; Bagryanskaya, E. G. *Appl. Magn. Reson.* **2011**, *41*, 383−392.

(12) (a) Ivachtchenko, A. V.; Kravchenko, D. V.; Zheludeva, V. I.; Pershin, D. G. *J. Heterocycl. Chem.* **2004**, *41*, 931−940. (b) Zhao, Z.-G.; Wang, Z.-X. *Synth. Commun.* **2007**, *37*, 137−147.

(13) (a) Finar, I. L.; Lord, G. H. *J. Chem. Soc.* **1957**, 3314−3315. (b) Potapov, A. S.; Khlebnikov, A. I.; Ogorodnikov, V. D. *Russ. J. Org. Chem.* **2006**, *42*, 550−554. (c) European Patent 1762568 (A1).

(14) Bertrand, J. A.; Kaplan, R. I. *Inorg. Chem.* **1966**, *5*, 489−491.

(15) Sviridenko, F. B.; Stass, D. V.; Kobzeva, T. V.; Tretyakov, E. V.; Klyatskaya, S. V.; Mshvidobadze, E. V.; Vasilevsky, S. F.; Molin, Yu. N. *J. Am. Chem. Soc.* **2004**, *126*, 2807−2819.

(16) Reijerse, E.; Schmidt, P. P.; Klihm, G.; Lubitz, W. *Appl. Magn. Reson.* **2007**, *31*, 611−626.